Research Square

Preprints are preliminary reports that have not undergone peer review.
They should not be considered conclusive, used to inform clinical practice,
or referenced by the media as validated information.

Analysis of Reduced-Representation DNA Methylome and Transcriptome in Spontaneous Primary Age-related Cataract of Microtus fortis

Ruotong Guan
Xiangya Medical College
Zhangyi Liu
Xiangya Medical College
Jing Zhang
Xiangya Medical College
Tianqiong He
hetianqiong@csu.edu.cn
Xiangya Medical College
Zhijun Zhou
Xiangya Medical College

Article

Keywords: DNA methylation, RRBS, RNA-seq, age-related cataract, Microtus fortis

Posted Date: November 5th, 2026

DOI: https://doi.org/10.21203/rs.3.rs-10637203/v1

License: This work is licensed under a Creative Commons Attribution 4.0 International License.
Read Full License

Additional Declarations: No competing interests reported.

Abstract

Cataract is a major cause of visual impairment worldwide, and the underlying pathogenesis is not yet fully understood. In this study, the DNA methylation and transcription profiles of lens of primary age-related cataract (ARC) and healthy *M. fortis* were generated by reduced representation bisulfite sequencing (RRBS) and RNA sequencing (RNA-seq), to identify potential epigenetic biomarkers of ARC. Compared with the healthy *M. fortis*, 1903 significantly hypermethylated and 15297 hypomethylated differentially methylated regions (DMRs) were identified in the lens of cataract *M. fortis.* Pathway enrichment analyses reveal these DMR-associated genes were mainly enriched in nervous-related pathways, small guanosine triphosphatases (GTPase) binding, actin binding, wnt signaling pathway and calcium signaling pathway. And transcriptome analysis revealed 5792 DEGs in the cataract *M. fortis* compared with healthy *M. fortis*, including 3218 significantly upregulated and 2574 significantly downregulated genes. These DEGs were mainly enriched in ribosome-related pathways, JAK-STAT signaling pathway, and cytoskeleton in muscle cells. Furthermore, 147 upregulated genes with promoter hypomethylation and 51 downregulated genes with promoter hypermethylation in their promoter regions were obtained by integrated analysis of methylome and transcriptome. And these DEGs were mainly enriched in hypoxia-inducible factor-1 (HIF-1) signaling pathway, ferric iron binding, actin binding, small GTPase binding and JAK-STAT signaling pathway. Moreover, IGV results showed multiple genes including chemokine C-X-C motif Ligand 1 (*CXCL1)*, granulocyte colony-stimulating factor (*CSF3)*, transferrin (*TF)* and *RHOB* genes exhibited markedly lower methylation levels in promoter regions, and transcription of these genes was upregulated in lens of cataract *M. fortis*. Crystallin gamma C (*CRYGC)*, gap junction protein alpha 3 (*GJA3*) genes exhibited markedly higher methylation levels in the cataract group, and the transcription of these genes in the cataract group was significantly lower than that in the control group. As a result, our findings indicated that aberrant DNA methylation is closely associated with the cataract formation and might provide a basis for future mechanistic studies of ARC.

1 Introduction

Cataract, opacification of the lens, is the leading cause of blindness worldwide [1]. And multiple risk factors contribute to cataract development, including aging, genetic composition, smoking, diabetes mellitus, exposure to ultraviolet light, calcium imbalance and oxidative stress [2, 3]. In addition, ARC is the most prevalent type being responsible for 48% of blindness [4, 5]. To date, the only treatment for cataracts is to extract the cataractous lens and implant an artificial intraocular lens. However, this procedure carries considerable risks, including posterior capsule rupture, postoperative inflammation, and intraocular lens dislocation [6]. Moreover, as the exact molecular mechanisms underlying cataract remain poorly understood, the development of diagnosis, management, and effective therapies for cataract was limited. Cataract continues to be a leading public-health issue that will grow in importance as the life expectancy is extended worldwide.

As is known, DNA methylation is a crucial epigenetic modification that regulates gene expression through heritable regulatory mechanisms, thereby regulating diverse physiological processes and

disease progression [7]. Accumulating evidence has suggested that abnormal DNA methylation is implicated in cataract pathogenesis and lens development [8–10]. For instance, DNA hypermethylation of CpG islands in the *COL4A1* promoter reduces *COL4A1* expression in ultraviolet B (UVB)-exposed human lens epithelial cells (hLECs) and rats anterior lens capsules, which in turn suppresses cell proliferation and promotes apoptosis [11]. DNA methylation-mediated downregulation of *WRN* will inhibit oxidative stress-induced apoptosis of hLECs through ATM/p53 signaling pathway, ultimately affecting the ARC formation [12]. In the lens of age-related nuclear cataract (ARNC) induced by the UVB, hypermethylation at the special locus of *ERCC6* promoter leads to reduced *ERCC6* expression and impaired DNA damage repair capacity in the lens [13]. Furthermore, the expression of *DNMT3B*, *HDAC1*, *HDAC4*, *HDAC9*, and *MBD3* genes are elevated in LECs of ARC may be involved in epigenetic modifications [14]. However, the detailed molecular mechanisms of DNA methylation in ARC development have not been fully clarified. Therefore, comprehensive exploration of the epigenetic regulatory mechanisms of DNA methylation in ARC development is of great significance.

Microtus fortis (*M. fortis*), also known as the reed vole or Yangtze vole, is mainly distributed across the Dongting Lake wetland in China, Russia, North Korea and Mongolia close to the northeast borderlands of China [15]. It's well-known that *M. fortis* is a natural nonpermissive host that has exhibited intrinsic resistance against *Schistosoma japonicum* (*S. japonicum*) infection, which is an ideal experimental animal model has been widely used in the research against *S. japonicum* infection [16]. Besides, *M. fortis* serves as a significant rodent model that exhibits additional traits including digestion-metabolism, ovarian cancer, reproductive biology, behavior, and species evolution [17]. During the experimental breeding of *M. fortis*, we first found that individuals aged 12 months or older spontaneously develop cataract with an approximate incidence rate of 20% [18]. It has been reported that the average lifespan of *M. fortis* in the Dongting Lake area is approximately one year (slightly longer under laboratory conditions) [19]. Consistently, human ARC predominantly occurs in people over 50 years old with a high incidence rate [20]. These findings confirm that spontaneous cataract in *M. fortis* is strongly age-dependent, indicating that this species may serve as a promising natural animal model for human ARC research.

In the present study, we isolated lenses from 13-month-old male *M. fortis* with spontaneous cataract and age-matched healthy males. RRBS was performed to profile genome-wide DNA methylation in lens tissues. Combined with transcriptome sequencing data, we conducted GO and KEGG enrichment analyses to elucidate the regulatory roles of DNA methylation in the lens of cataract *M. fortis*. Taken together, our study will illustrate the epigenetic basis of spontaneous cataract in *M. fortis* and lay a foundation for the development of candidate targets for ARC.

2 Materials and Methods

Ethics statement

Animal experiment protocols were approved by the Laboratory Animal Welfare and Ethics Committee of Central South University (Changsha, China; approval no. CSU-2026-0020).

Animals and sample preparation

M. fortis, were obtained from Xiangya Medical College, Central South University (Changsha, China). In this study, a total of five male healthy *M. fortis* and five male *M. fortis* aged 13-15 months old with cataract (weighing 70-80g) were assigned to the control and the experimental groups, respectively. The animals were anesthetized by 3% isoflurane and then the lenses were removed. The lens from one eye of each *M. fortis* was collected. Samples were stored in an ultra-low temperature freezer (−80°C). Finally, all animals were euthanized by CO_2 inhalation. RRBS and RNA-seq samples were derived from the same side of the lens of *M. fortis*.

Slit-lamp examination

Animals were anesthetizedand then the pupils were dilated using Compound Tropicamide Eye Drops (Wuhan Wujing Pharmaceutical Co., Ltd.). Lens opacity was then observed under a Small Animal In Vivo Vascular Imaging System (Phoenix, USA).

RRBS

The RRBS libraries were constructed by WiseBio Co. Ltd. Genomic DNA from lens samples was extracted by TIANamp Genomic DNA Kit (TIANGEN) following the manufacturer's protocols. About 1μg of genomic DNA mixed with unmethylated lambda DNA was digested by MspI enzyme. After digestion, the libraries were constructed as the Illumina paired-end protocol with some modifications. Briefly, purified digested DNA was subsequently treated with a mix of T4 DNA polymerase, Klenow Fragment and T4 polynucleotide kinase to repair, blunt and phosphorylate ends. After that, the blunt DNA were 3' adenylated using Klenow Fragment (3'-5' exo-) and following with ligation to adaptors synthesized with 5'-methylcytosine instead of cytosine using T4 DNA Ligase. After each step, the DNA was purified using MinElute PCR Purification Kit (Qiagen). ZYMO EZ DNA Methylation-Gold Kit™ was employed to convert unmethylated cytosine into uracil according to the instructions and the PCR was carried out. Before analysis with Illumina sequencing platform, the size selected library was analyzed by the Bioanalyzer analysis system (Agilent, Santa Clara, USA) [21].

RNA-seq

The RNA-seq libraries were constructed by WiseBio Co. Ltd as follows. Briefly, the total RNA of each sample was extracted using Invitrogen TRIzol® Reagent and then treated with RNase-free DNase I for 30 min according to the manufacturer's protocols. The poly(A) containing mRNA were purified using Oligo(dT) Beads from about 1 μg total RNA. The captured mRNA was firstly fragmented into 100-200nt using divalent cations at elevated temperature. The fragmented mRNA was reverse-transcribed with SuperScript II and then converted to double-stranded cDNA using RNase H and DNA Pol I by random priming. After purification, the double-stranded cDNA was subjected to blunt-ending, dA addition to 3'-end and adapter ligation. Finally, PCR was carried out to enrich the adapter ligated cDNA and the libraries

were analyzed by Agilent Bioanalyzer 2100 and quantified by qPCR before sequencing by the Illumina sequencing platform.

Data analysis and Functional Enrichment Analysis

Adapter sequences were trimmed by using cutadapt. The parameter settings used were "-a AGATCGGAAGAGC -m 35 -n 2". The cleaned reads were mapped back to genome using BSMAP software version 2.90 [22]. The parameter settings used were "-n 0 -v 0.08 -g 1". Methylation ratios were extracted from BSMAP output (SAM) using a Python script (methratio.py) which is distributed with the BSMAP package. Only unique mapped reads were used to calculate methylation ratios. Only cytosines in a CpG context with sufficient sequencing depth (greater than or equal to 5x coverage) were retained for further analysis. Differentially methylated cytosines (DMCs) were detected using MethylKit (v1.20) in de-novo mode among CpG sites with at least 5x coverage [23]. The parameter settings used were "--mincov 5 --m_cutoff 0.1 --q_cutoff 0.05". Differentially methylated regions (DMRs) were detected using metilene in de-novo mode among CpG sites with at least 5x coverage [24]. The parameter settings used were "--mincpgs 4 --minMethDiff 0.2 --mtc 1 -X 1 -Y 1 -v 0.7". Then detected DMR were filtered according to the standard: (1) Q-value must be less than 0.01; (2) methylation level difference must be greater than 0.2; (3) CpG number contained in DMR must be greater than 4; (4) the length of the DMR must be greater than 50 bp. The related genes were then subjected to enrichment analysis of GO and KEGG by clusterProfiler.

Quality control of raw reads was performed using FastQC (version 0.12.1) (https://www.bioinformatics.babraham.ac.uk/projects/fastqc/), and clean reads were obtained following the removal of low-quality reads with Trimmomatic (version 0.38) software [25]. The parameter settings used were "HEADCROP:8 LEADING:3 TRAILING:3 SLIDINGWINDOW: 4: 15 MINLEN: 36". Hisat2 (v2.2.1) was employed for performing read mapping to *M. fortis* genome reference (GWHESEF00000000) [26]. Gene expression profiling was based on the number of reads. TPM (Transcripts Per Kilobase of exon model per Million mapped reads) values were calculated by StringTie (v2.1.7), and were used to estimate the expressed values [27]. DEGs were obtained using DEseq2 (v1.34.0) with a p value < 0.05 and an absolute log2(fold-change) > 1. KEGG and GO enrichment analysis was performed on the clusterProfiler R package (v4.4.2) [28, 29]. Furthermore, the DMR annotation results of CGs in the promoter region and gene body region were combined with the DEGs results for VENN analysis and single-sample gene wide association analysis.

3 Results

Increased DNA Methylation Levels in the Lens of *M. fortis* During the Development of Cataract

Slit-lamp examination revealed that the lenses of *M. fortis* in the control group were brown and transparent (Figure 1A), whereas those of cataractous *M. fortis* in the experimental group exhibited white opacification (Figure 1B). To explore the role of DNA methylation in cataract progression, we isolated lenses from cataract and healthy *M. fortis* and profiled DNA methylation using RRBS. Each sample

generated over 77.37 million clean reads (7.5 Gb), with a mapping rate to the reference genome above 81.82% and a bisulfite conversion efficiency exceeding 99% (Table 1), indicating high data integrity and accuracy. Principal component analysis (PCA) and hierarchical clustering (HC) showed distinct DNA methylation patterns between the cataract group and the control group(Figure 2A and B). DNA methylation mainly occurred at CG cytosine sites (mean methylation level, m = 63.03%) (Figure 2C). Most differential CG sites were mainly located in regions 2-kb upstream of the gene body (promoter region) (Figure 2D). To define the specific position of methylated sites in the promoter, the promoter was further divided into five gene functional regions: CGI-upshelf, CGI-upshore, CG islands (CGI), CGI-downshore, and CGI-downshelf. As depicted in Figure 2E, the cataract group showed significantly higher CG methylation levels in the CGI region than the control group. These data collectively suggested that the global DNA methylation levels were increased in lenses during the development of cataract.

Functional Enrichment of the DMR-associated genes Derived from DMRs in Lens of cataract *M. fortis*

Next, we attempted to explore the association between methylation and the pathogenesis of cataract by calculating the DMRs between cataract and the control group under the CpG contexts. In total, 17,200 DMRs were obtained (including 1903 significantly hyper- and 15297 hypomethylated DMRs) (Figure 3A). And more DMRs were localized in exons than in promoter regions (Figure 3B-C). GO enrichment analysis results showed DMGs in hypermethylated DMRs were significantly enriched in biological process (BP) such as multicellular organism development, nervous system development and neurogenesis. The top enriched cellular component (CC) included neuron projection, neuron part, somatodendritic compartment and cell body. For molecular function (MF), these genes were enriched in RNA polymerase □-specific, DNA-binding transcription factor activity, GTPase binding, beta-catenin binding and small GTPase binding (Figure 3D). DMGs in hypomethylated DMRs were mainly enriched in BP entries including nervous system development, anatomical structure morphogenesis, detection of chemical stimulus involved in sensory perception and neurogenesis. The corresponding CC were cell projection, plasma membrane bounded cell projection, neuron part and neuron projection. The enriched MF included olfactory receptor activity, structural constituent of ribosome, small GTPase binding and actin binding and protein binding (Figure 3E). KEGG pathway analysis showed DMGs in hypermethylated DMRs were enriched in Wnt signaling pathway, calcium signaling pathway, cGMP-PKG signaling pathway and Hippo signaling system (Figure 3F). DMGs in hypomethylated DMRs were associated with the calcium signaling pathway, MAPK signaling pathway, Rap1 signaling pathway, Ras signaling pathway and oxidative phosphorylation (Figure 3G).

Transcriptomic Profiling of Lens During the cataract Development of *M. fortis*

Given the regulatory effect of DNA methylation on gene expression, we performed RNA-seq to characterize transcriptomic changes in cataract development. After quality filtering, each sample yielded an average of 26,178,840 paired-end clean reads, with an average Q30 value of 96.56% and an overall mapping rate above 98% (Table 2). PCA and cluster analysis indicated a clear separation among the two groups (Figure 4A and B). A total of 5,792 DEGs were identified in the cataract *M. fortis* compared with

healthy *M. fortis*, comprising 3,218 significantly upregulated genes (e.g., *CCL2*, *ADAM28*, *CDKN2A*, *CXCL6*) and 2,574 significantly downregulated genes (e.g., *CRYGA*, *CRYGC*, *FOXG1*) (Table S1). The expression heatmap revealed noticeable differences in gene expression patterns between the two groups (Figure 4C).

Moreover, GO analysis indicated these downregulated DEGs were enriched in BP related in SRP-dependent cotranslational protein targeting to membrane, cotranslational protein targeting to membrane, establishment of protein localization to endoplasmic reticulum and protein localization to endoplasmic reticulum. The enriched CC included cytosolic ribosome, cytosolic part and ribosome subunit, and the MF were dominated by structural constituent of ribosome, structural molecule activity and olfactory receptor activity (Figure 4D). KEGG analysis revealed that the downregulated DEGs were enriched in oxidative phosphorylation, calcium signaling pathway, JAK-STAT signaling pathway and cytokine-cytokine receptor interaction (Figure 4E). Upregulated DEGs were enriched in BP such as immune system process, regulation of response to stimulus, translation and positive regulation of response to stimulus. The corresponding CC included ribonucleoprotein complex, extracellular region and ribosome, and the MF involved structural constituent of ribosome, signaling receptor binding, RNA binding and cell adhesion molecule binding (Figure 4F). KEGG pathways enriched for upregulated DEGs included oxidative phosphorylation, cytoskeleton in muscle cells, Rap1 signaling pathway, TNF signaling pathway and JAK-STAT signaling pathway (Figure 4G).

Correlation Analysis between DMRs and Genome-Wide Gene Expression

Since promoter methylation plays a critical role in transcriptional regulation, we focused on DMRs within gene promoter regions for integrated analysis. Venn diagram analysis identified 147 genes that were significantly upregulated and harbored hypomethylated DMRs in the promoters (Figure 5A, Table 3). GO analysis showed these genes were enriched in certain BP, including cell surface receptor signaling pathway, interleukin-4-mediated signaling pathway and immune system process, and in MF involved in phospholipase A2 activity, ferric iron binding, calcium-dependent phospholipid binding and cytokine binding, and in CC including extracellular region part, extracellular region, extracellular space and I-kappaB/NF-kappaB complex (Figure 5B). KEGG analysis further demonstrated enrichment in the JAK-STAT signaling pathway, sphingolipid signaling pathway, HIF signaling pathway and tight junction (Figure 5C). Meanwhile, 51 genes with hypermethylated DMRs in the promoters were significantly downregulated in the cataract group compared to the control group (Figure 5D, Table 4). GO analysis revealed these genes were enriched in BP including embryonic organ morphogenesis, regulation of ectoderm development and negative regulation of ectoderm development. The enriched CC included GABA receptor complex, cytosolic small ribosomal subunit and small ribosomal subunit, and the MF contained dynein heavy chain binding, metal ion binding and GTPase binding (Figure 5E). KEGG analysis showed that these genes were exclusively enriched in signaling pathways regulating pluripotency of stem cells (Figure 5F).

Identification of Key DNA Methylation-Regulated Genes Associated with cataract development in *M. fortis*

Integrative visualization of RRBS and RNA-seq was performed using the Integrative Genomics Viewer (IGV) to characterize epigenetic regulation of the identified genes. The results showed that the promoter region of *RHOB* (chr4: 15923586-15926016), *CSF3* (chr5: 79600108-79604024), *CXCL1* (chr11: 75989410-75992304), *TF* (chr2: 21757956-21804986) genes exhibited markedly lower methylation levels in the cataract group than in the control group. Correspondingly, the transcription of these genes in the cataract group was significantly higher than that in the control group (Figure 6 A-D). Moreover, *CRYGC* (chr1: 4882484-4884188), *GJA3* (chr17: 54475480-54497348) genes exhibited markedly higher methylation levels in the cataract group, and the transcription of these genes in the cataract group was significantly lower than that in the control group (Figure 6 E-G). These findings suggest that thesegenes may undergo altered expression in the cataract group in association with promoter methylation changes, leading to its aberrant expression.

4 Discussion

In this study, we profiled the DNA methylome landscape of cataract in *M. fortis* using RRBS, and the results confirmed the DNA methylation levels were increased in lens of cataract *M. fortis* compared with healthy *M. fortis*. Integrated methylome and transcriptome analysis revealed that DEGs with aberrant methylation were mainly enriched in HIF-1 signaling pathway, ferric iron binding, cytokine binding, GTPase binding and JAK-STAT signaling pathway. IGV results showed multiple genes including *CXCL1*, *CSF3, TF* and *RHOB* genes exhibited markedly lower methylation levels in promoter regions, and transcription of these genes was upregulated in lens of cataract *M. fortis*. *CRYGC*, *GJA3* genes exhibited markedly higher methylation levels in the cataract group, and the transcription of these genes in the cataract group was significantly lower than that in the control group. Our findings indicated that abnormal DNA methylation is tightly associated with the cataract development and provides valuable clues for developing novel therapeutic drugs for cataract.

Ras homolog gene family GTPases (Rho GTPases), a subfamily of the small G protein, contributes to actin cytoskeletal reorganization [30]. Inactivation of Rho-GTPases in developing lens fibers disrupts cell elongation and differentiation, resulting in disordered fiber cell migration and organization, as well as disrupted actin cytoskeletal organization. Accumulating evidence has proven that the actin cytoskeleton and actin-binding proteins contribute to ARC pathogenesis by inducing abnormal lens fiber cell elongation and differentiation. Therefore, Rho GTPases are essential as the actin cytoskeleton for lens fiber cell elongation and differentiation [31]. *RHOB*, a member of the Rho subfamily of small GTPases, regulates cytoskeletal reorganization, cell cycle regulation, growth factor receptor trafficking and apoptosis. Previous studies have reported specific expression of *RHOB* in the lens during early eye development, implying its potential role in cytoskeletal reorganization associated with lens epithelial cell elongation and differentiation [32]. Consistent with the previous studies, the expression of *RHOB* (log2 FoldChange = 2.77) was upregulated in lens of cataract *M. fortis*, and hypomethylation of the *RHOB*

promoters (methyl-diff=-0.2) were observed in our study. Furthermore, GO enrichment analysis results indicated the hypomethylated DMGs were enriched in actin binding and small GTPase binding. Thus, we speculated actin binding proteins and Rho GTPases were also critical for lens fiber cell elongation and differentiation in *M. fortis*, and further investigations into the methylation regulatory mechanism and biological function of *RHOB* gene are warranted.

GO and KEGG analyses identified the DMGs were associated with the HIF-1α signaling pathway, Wnt signaling pathway, Rap1 signaling pathway and calcium signaling pathway, which have also been reported to be altered in human ARC with abnormal methylation [33]. The Rap1 signaling pathway plays an important role in the lens epithelial phenotype and morphology, as well as in the retinal and choroidal vasculature [34]. Wnt/β-catenin signaling activity is required for proper lens fiber cell differentiation and lens transparency during later stages of lens development [35]. HIF-1α inhibits cell apoptosis and alleviates lens opacification, and presumably plays a key role in protecting lenses from diabetic cataract [36]. Earlier studies using mouse ARC models and performed DNA methylation and transcriptome sequencing analyses to find epigenetic indicators for ARC, and found the HIF-1 signaling pathway were enriched [5]. In addition, high glucose promotes HuLEC calcification via the activation of the HIF-1 signaling pathway [37]. Quercetin is a dietary bioflavonoid which has been shown to activates the HIF-1 signaling pathway in human lens epithelial cells to inhibit lens opacification in multiple cataract models [38]. These results are in accordance with our study, a series of DEGs with abnormal methylation were involved in HIF-1 signaling pathway. Although direct evidence linking the HIF-1 signaling pathway to ARC remains limited, we speculated HIF-1 signaling pathway may play a role in ARC development, which requires more experiments to explore.

Inflammatory and immune responses have been implicated in cataract development. The JAK-STAT signaling pathway has been implicated in cataract pathogenesis [39]. With increasing severity of nuclear cataract, there is a significant increase in proinflammatory cytokines such as Chemokine (C-C motif) ligand 2 (CCL2), CXCL10, IL-8, and VEGF-A [40]. Higher CCL2 expression is correlated with the development of early postoperative corneal edema in diabetic patients [41]. In mouse cataract surgery models, chemokines including CXCL1, *CSF3* are recruited to the lens post-wounding [42, 43]. Herein, multiple DEGs with aberrant methylation (e.g, IL4R, CSF3, SOCS1, STAT6) were enriched in the JAK-STAT signaling pathway. Notably, the expression of *CCL2* gene was the most upregulated (log2 FC = 13.58) in cataract *M. fortis.* Additionally, IGV results showed multiple genes including *CXCL1*, *CSF3, TF* and *RHOB* genes exhibited markedly lower methylation levels in promoter regions, and transcription of these genes was upregulated in lens of cataract *M. fortis*. Collectively, our data support that the immune response and inflammation contribute to cataract development of *M. fortis*.

Furthermore, IGV results showed *CRYGC*, *GJA3* genes exhibited markedly higher methylation levels in the cataract group, and the transcription of these genes in the cataract group was significantly lower than that in the control group. In addition, crystallin proteins, including α-, β- and γ-crystallins, represent about 90% of lens soluble proteins in human. These proteins play critical roles in the optical transparency and high refractive index. Only two members, CRYGC and CRYGD, encode abundant lens γ-crystallins in

humans, which comprise about 25% in the human lens. CRYGC is present in the central nucleus region of the lens and is associated with autosomal dominant cataract [44]. The *GJA3* gene encodes the CX46 protein, which is critical to maintain the ionic and water balance and transparency and optical properties of the lens. More than 30 GJA3 variants are reported to be associated with congenital cataracts, which makes GJA3 one of the most frequently mutated genes related to lens opacity [45]. Su et al found that downregulation of GJA3 in LEC was associated with ARC genesis through interference with H_2O_2-induced LEC apoptosis[46]. Moreover, we previously found that the expression of GJA3 was downregulated in lens of cataract *M. fortis* compared with healthy *M. fortis* [18]. In this study, we found *GJA3* gene exhibited markedly higher methylation levels in the cataract group. Therefore, we speculated the downregulated expression of *GJA3* gene correlated with abnormal methylation, and was strongly associated with cataract pathogenesis in *M. fortis*. Taken together, we speculated differential expression and methylation of these genes in cataract *M. fortis* were highly linked to ARC progression. Further exploration of the biological functions of these genes and regulatory mechanisms will provide a theoretical basis for discovering new therapeutic targets for ARC.

5 Conclusion

In this study, we profiled the DNA methylome landscape and transcription profiles of cataract in *M. fortis* and using RRBS and RNA seq, respectively. And integrated methylome and transcriptome analysis revealed that 198 DEGs with aberrant methylation were mainly enriched in HIF-1 signaling pathway, ferric iron binding, cytokine binding, GTPase binding and JAK-STAT signaling pathway. Furthermore, IGV results found multiple genes including *CXCL1*, *CSF3, TF* and *RHOB* genes exhibited markedly lower methylation levels in promoter regions, and transcription of these genes was upregulated in lens of cataract *M. fortis*. *CRYGC*, *GJA3* genes exhibited markedly higher methylation levels in the cataract group, and the transcription of these genes in the cataract group was significantly lower than that in the control group. As a result, our findings indicated that abnormal DNA methylation is tightly associated with the cataract development and provides valuable clues for developing novel therapeutic drugs for cataract.

Declarations

Acknowledgements

Not applicable.

Funding

This work was supported by grants from the Hunan Provincial Key Research and Development Program (2024DK2001), Natural science foundation of Hunan province (2024JJ5422, 2024JJ6494).

Author information

Authors and Affiliations

Department of Laboratory Animal Science, Xiangya Medical College; Changsha, Hunan, China 410013

Ruotong Guan, Zhangyi Liu, Jing Zhang, Tianqiong He, Zhijun Zhou

Hunan Key Laboratory of Animal Models for Human Diseases, Central South University, Changsha, Hunan, China 410013

Ruotong Guan, Zhangyi Liu, Jing Zhang, Tianqiong He, Zhijun Zhou

*** Corresponding Author**

Correspondence to Tianqiong He

Ethics declarations

Ethics approval and consent to participate

This animal study protocol was approved by theLaboratory Animal Welfare and Ethics Committee of Central South University (Changsha, China; approval no. CSU-2026-0020)**.**

Consent for publication

Not applicable.

Data availability statement

All data generated or analyzed during this study are included in this published article [and its supplementary information files].

Competing interests

The authors declare no competing interests.

References

1. Świerczyńska, M., Tronina, A. & Smędowski, A. Understanding cataract development in axial myopia: The contribution of oxidative stress and related pathways. *Redox Biol.* **80**, 103495 (2025).
2. Kulbay, M., Wu, K. Y., Nirwal, G. K., Bélanger, P. & Tran, S. D. Oxidative Stress and Cataract Formation: Evaluating the Efficacy of Antioxidant Therapies. *Biomolecules* **14**(9). (2024).
3. Borges-Rodríguez, Y., Morales-Cueto, R. & Rivillas-Acevedo, L. Effect of the Ultraviolet Radiation on the Lens. *Curr. Protein Pept. Sci.* **24** (3), 215–228 (2023).
4. Caixinha, M., Santos, J., Santos, M. & Nunes, S. Animal model for in-vivo Nuclear Cataract. Lens hardness and elasticity assessment. *J. Mech. Behav. Biomed. Mater.* **157**, 106610 (2024).

5. Hu, Y. et al. Genome-wide DNA methylation and transcriptome sequencing analyses of lens tissue in an age-related mouse cataract model. *PLoS One*. **20** (1), e0316766 (2025).
6. Bhandari, S. & Chew, E. Y. Cataract surgery and the risk of progression of macular degeneration. *Curr. Opin. Ophthalmol.* **34** (1), 27–31 (2023).
7. Michalak, E. M., Burr, M. L., Bannister, A. J. & Dawson, M. A. The roles of DNA, RNA and histone methylation in ageing and cancer. *Nat. Rev. Mol. Cell. Biol.* **20** (10), 573–589 (2019).
8. Wang, L., Li, P. & Guo, X. Screening of methylation genes in age-related cataract. *Int. J. Ophthalmol.* **11** (7), 1102–1107 (2018).
9. Wang, Y. & Guan, H. The Role of DNA Methylation in Lens Development and Cataract Formation. *Cell. Mol. Neurobiol.* **37** (6), 979–984 (2017).
10. Yang, W. et al. Aging of the human eye lens: Epigenetic landscape and therapeutic targets in age–related cataracts (Review). *Int J. Mol. Med* **56**(6). (2025).
11. Wang, L. et al. DNA hypermethylation of COL4A1 in ultraviolet-B-induced age-related cataract models in vitro and in vivo. *Int. J. Ophthalmol.* **17** (10), 1791–1799 (2024).
12. Jiang, S. & Chen, J. WRN inhibits oxidative stress-induced apoptosis of human lensepithelial cells through ATM/p53 signaling pathway and its expression is downregulated by DNA methylation. *Mol. Med.* **26** (1), 68 (2020).
13. Wang, Y., Li, F., Zhang, G., Kang, L. & Guan, H. Ultraviolet-B induces ERCC6 repression in lens epithelium cells of age-related nuclear cataract through coordinated DNA hypermethylation and histone deacetylation. *Clin. Epigenetics*. **8**, 62 (2016).
14. Wang, Y., Zhang, G., Kang, L. & Guan, H. Expression Profiling of DNA Methylation and Transcriptional Repression Associated Genes in Lens Epithelium Cells of Age-Related Cataract. *Cell. Mol. Neurobiol.* **37** (3), 537–543 (2017).
15. Jia, S., Suoyu, X., Mei, P., Zhijun, Z. & Zhongdao, W. Mechanisms of Resistance to Schistosoma japonicum Infection in Microtus fortis, the Natural Non-permissive Host. *Front. Microbiol.* **11**, 2092–2092 (2020).
16. Jia, S. et al. Macrophage-mediated trogocytosis contributes to destroying human schistosomes in a non-susceptible rodent host, Microtus fortis. *Cell. discovery*. **9** (1), 101–101 (2023).
17. Zhang, D. et al. The Microtus fortis chromosome-level genome: illuminating adaptive evolution and natural parasite immunity. *BMC Genom.* **27** (1), 290–290 (2026).
18. He Tianqiong, Z. et al. Xia Xiaobo, Zhou Zhijun. Identification of spontaneous age-related cataract in Microtus fortis. *J. Cent. South. Univ. (Medical Science)*. **49** (04), 553–561 (2024).
19. Xin, L. V., Hong-zhong, D. E. N. G., Yong, L. I., Jun, W. U. & Yue-jin, T. A. N. Modeling and Simulation Analysis on Growth and Catastrophe of Microtus Fortis in Dong Ting Lake Area. *J. Syst. Simul. 2008*, **20**(23):6575–6579 ; 10.16182/j.cnki.joss.2008.23.023
20. Asbell, P. A. et al. Age-related cataract. *Lancet* **365** (9459), 599–609 (2005).

21. Sun, M. et al. Integrated DNA Methylation and Transcriptomics Analyses of Lacrimal Glands Identify the Potential Genes Implicated in the Development of Sjögren's Syndrome-Related Dry Eye. *J. Inflamm. Res.* **16**, 5697–5714 (2023).
22. Xi, Y. & Li, W. BSMAP: whole genome bisulfite sequence MAPping program. *BMC Bioinform.* **10**, 232 (2009).
23. Akalin, A. et al. methylKit: a comprehensive R package for the analysis of genome-wide DNA methylation profiles. *Genome Biol.* **13** (10), R87 (2012).
24. Jühling, F. et al. metilene: fast and sensitive calling of differentially methylated regions from bisulfite sequencing data. *Genome Res.* **26** (2), 256–262 (2016).
25. Bolger, A. M., Lohse, M. & Usadel, B. Trimmomatic: a flexible trimmer for Illumina sequence data. *Bioinformatics* **30** (15), 2114–2120 (2014).
26. Kim, D., Paggi, J. M., Park, C., Bennett, C. & Salzberg, S. L. Graph-based genome alignment and genotyping with HISAT2 and HISAT-genotype. *Nat. Biotechnol.* **37** (8), 907–915 (2019).
27. Pertea, M., Kim, D., Pertea, G. M., Leek, J. T. & Salzberg, S. L. Transcript-level expression analysis of RNA-seq experiments with HISAT, StringTie and Ballgown. *Nat. Protoc.* **11** (9), 1650–1667 (2016).
28. Love, M. I., Huber, W. & Anders, S. Moderated estimation of fold change and dispersion for RNA-seq data with DESeq2. *Genome Biol.* **15** (12), 550 (2014).
29. Wu, T. et al. clusterProfiler 4.0: A universal enrichment tool for interpreting omics data. *Innov. (Camb)*. **2** (3), 100141 (2021).
30. Mosaddeghzadeh, N. & Ahmadian, M. R. The RHO Family GTPases: Mechanisms of Regulation and Signaling. *Cells* **10**(7). (2021).
31. Karakosta, C., Samiotaki, M., Panayotou, G., Papakonstantinou, D. & Moschos, M. M. Role of actin-binding proteins in cataract formation. *Cytoskeleton (Hoboken)*. **82** (3), 98–110 (2025).
32. Maddala, R., Peng, Y. W. & Rao, P. V. Selective expression of the small GTPase RhoB in the early developing mouse lens. *Dev. Dyn.* **222** (3), 534–537 (2001).
33. Chen, X. et al. Preliminary study on whole genome methylation and transcriptomics in age-related cataracts. *Gene* **898**, 148096 (2024).
34. Ramos, C. J., Lin, C., Liu, X. & Antonetti, D. A. The EPAC-Rap1 pathway prevents and reverses cytokine-induced retinal vascular permeability. *J. Biol. Chem.* **293** (2), 717–730 (2018).
35. Antosova, B. et al. Ectopic activation of Wnt/β-catenin signaling in lens fiber cells results in cataract formation and aberrant fiber cell differentiation. *PLoS One*. **8** (10), e78279 (2013).
36. Han, X. et al. HIF-1α SUMOylation affects the stability and transcriptional activity of HIF-1α in human lens epithelial cells. *Graefes Arch. Clin. Exp. Ophthalmol.* **253** (8), 1279–1290 (2015).
37. Ababneh, H. et al. High glucose promotes osteogenic differentiation of human lens epithelial cells through hypoxia-inducible factor (HIF) activation. *J. Cell. Physiol.* **239** (5), e31211 (2024).
38. Radreau, P., Rhodes, J. D., Mithen, R. F., Kroon, P. A. & Sanderson, J. Hypoxia-inducible factor-1 (HIF-1) pathway activation by quercetin in human lens epithelial cells. *Exp. Eye Res.* **89** (6), 995–1002

(2009).

39. Zhao, Y. et al. Cross-talk of Signaling Pathways in the Pathogenesis of Allergic Asthma and Cataract. *Protein Pept. Lett.* **27** (9), 810–822 (2020).
40. Latz, C., Licht, A., Mirshahi, A., Latz, E. & Zimmer, K. Prospective Cytokine Profiling in Aqueous Humor Reveals a Proinflammatory Microenvironment in Highly Dense Nuclear Cataracts. *Invest. Ophthalmol. Vis. Sci.* **65** (11), 25 (2024).
41. Mitrović, S., Kelava, T., Šućur, A. & Grčević, D. Levels of Selected Aqueous Humor Mediators (IL-10, IL-17, CCL2, VEGF, FasL) in Diabetic Cataract. *Ocul Immunol. Inflamm.* **24** (2), 159–166 (2016).
42. Stepp, M. A. & Menko, A. S. Immune responses to injury and their links to eye disease. *Transl Res.* **236**, 52–71 (2021).
43. Jiang, J., Shihan, M. H., Wang, Y. & Duncan, M. K. Lens Epithelial Cells Initiate an Inflammatory Response Following Cataract Surgery. *Invest. Ophthalmol. Vis. Sci.* **59** (12), 4986–4997 (2018).
44. Shanbagh, S. et al. Distinct gene expression profiles underlie morphological and etiological differences in pediatric cataracts. *Indian J. Ophthalmol.* **71** (5), 2143–2151 (2023).
45. Tang, X-J., Shentu, X-C., Tang, Y-L., Ping, X-Y. & Yu, X-N. The impact of GJA3 SNPs on susceptibility to age-related cataract. *Int. J. Ophthalmol.* **12** (6), 1008–1011 (2019).
46. Su, D. et al. Down-regulation of GJA3 is associated with lens epithelial cell apoptosis and age-related cataract. *Biochem. Biophys. Res. Commun.* **484** (1), 159–164 (2017).

Tables

Tables 1 to 4 are available in the Supplementary Files section.

Figures

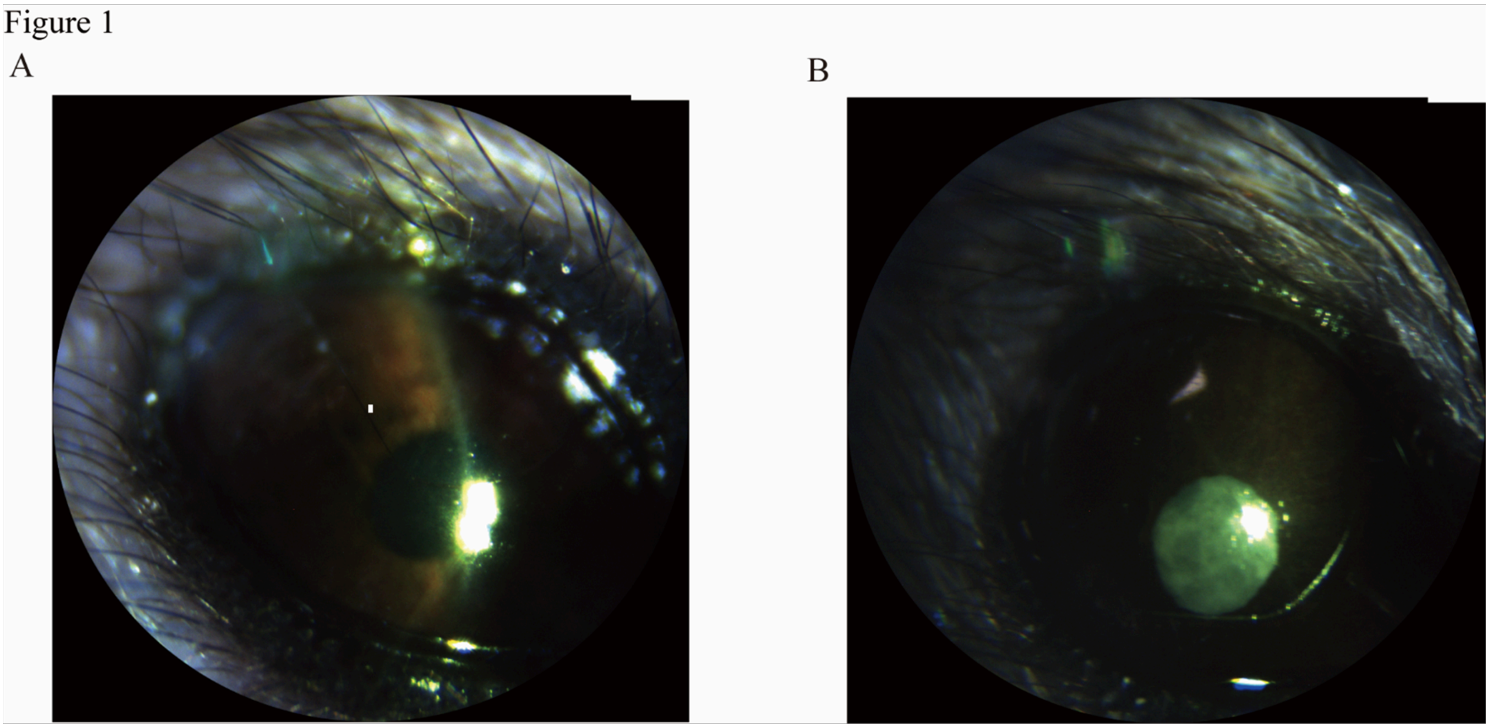


Figure 1

Photograph of slit-lamp examination. (**A**) Slit-lamp examination revealed the lenses were transparent in healthy *M. fortis* at 13-month-old. (**B**) Hypermature cataracts were observed in lenses of M. fortis with cataract at 13-month-old.

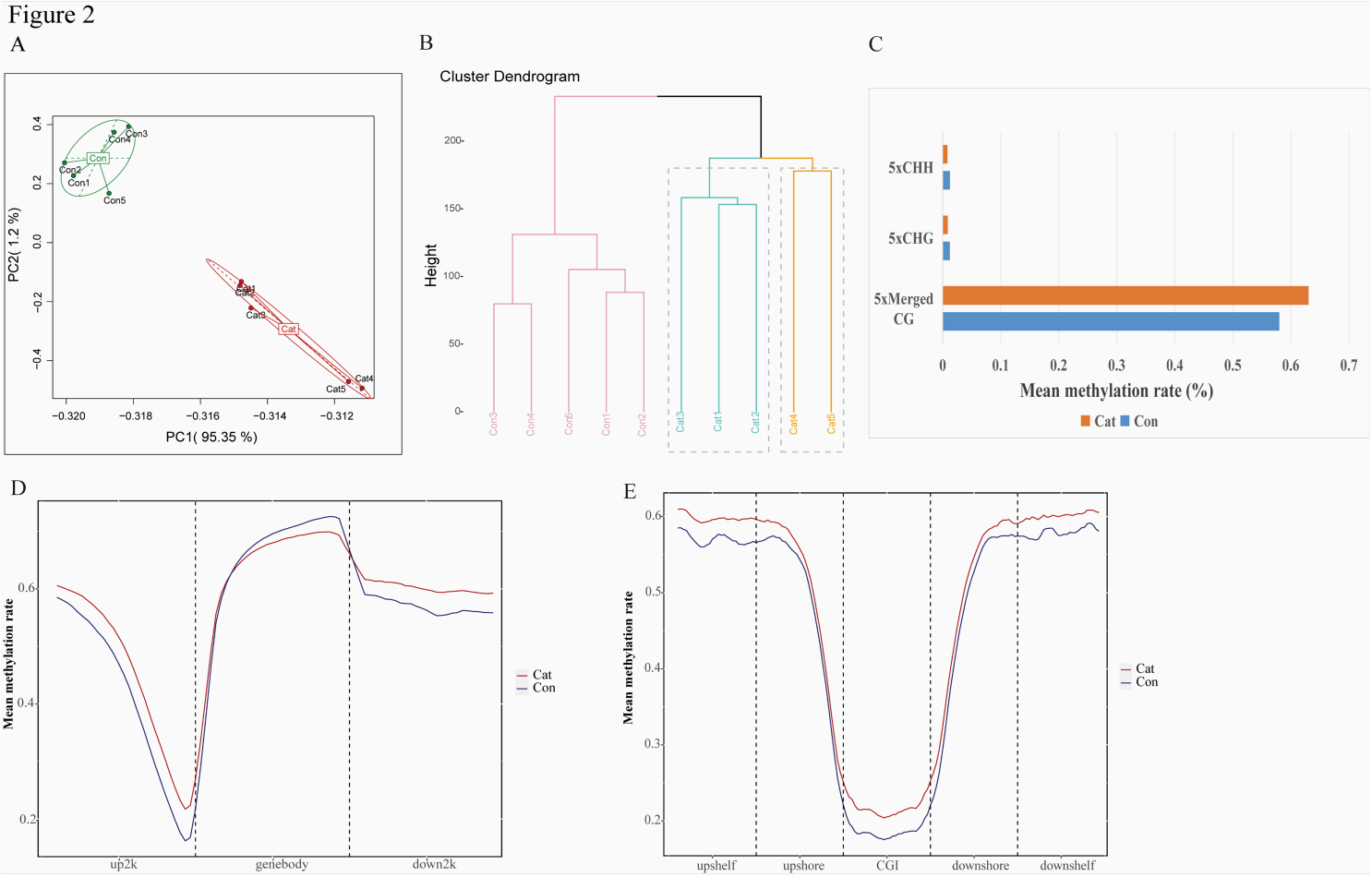


Figure 2

Elevated DNA methylation levels in lens of cataract*M. fortis*. (**A**) PCA based on individual cytosines. (**B**) HC analysis based on methylation levels at CpG sites. (**C**) DNA methylation rate under the contexts of CG, CHG, and CHH in *M. fortis* detected by RRBS. (**D**) DNA methylation levels along the gene body, 2-kb upstream of the TSS and 2-kb downstream of the TES for all genes. (**E**) DNA methylation levels of promoter CpG islands and surrounding areas.

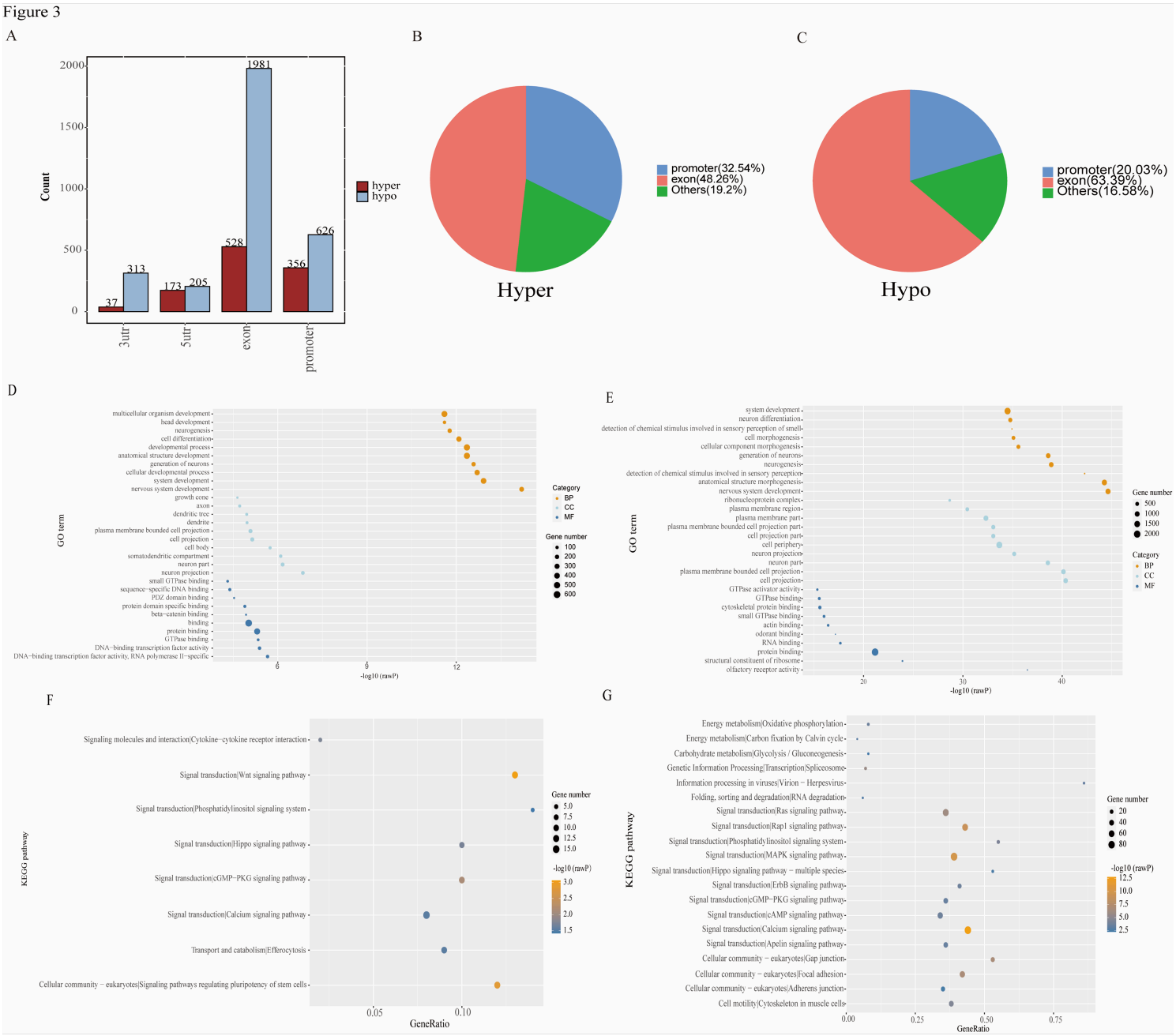


Figure 3

Functional enrichment analysis of genes associated with DMRsin lens of cataract *M. fortis*. (**A**) Statistics of hyper- and hypo-methylated DMRs in cataract *M. fortis* versus healthy *M. fortis*under CpG contexts. (**B**) DMRs distribution on different chromosomes. (**C**) The genomic location (exons, promoters and others) of identified hyper- and hypo-methylated DMRs. (**D**) GO enrichment analysis for hypermethylated DMR-associated genes. (**E**) GO enrichment analysis for hypomethylated DMR-associated genes. (**F**) KEGG pathway analysis for hypermethylated DMR-associated genes. (**G**) KEGG pathway analysis for hypomethylated DMR-associated genes.

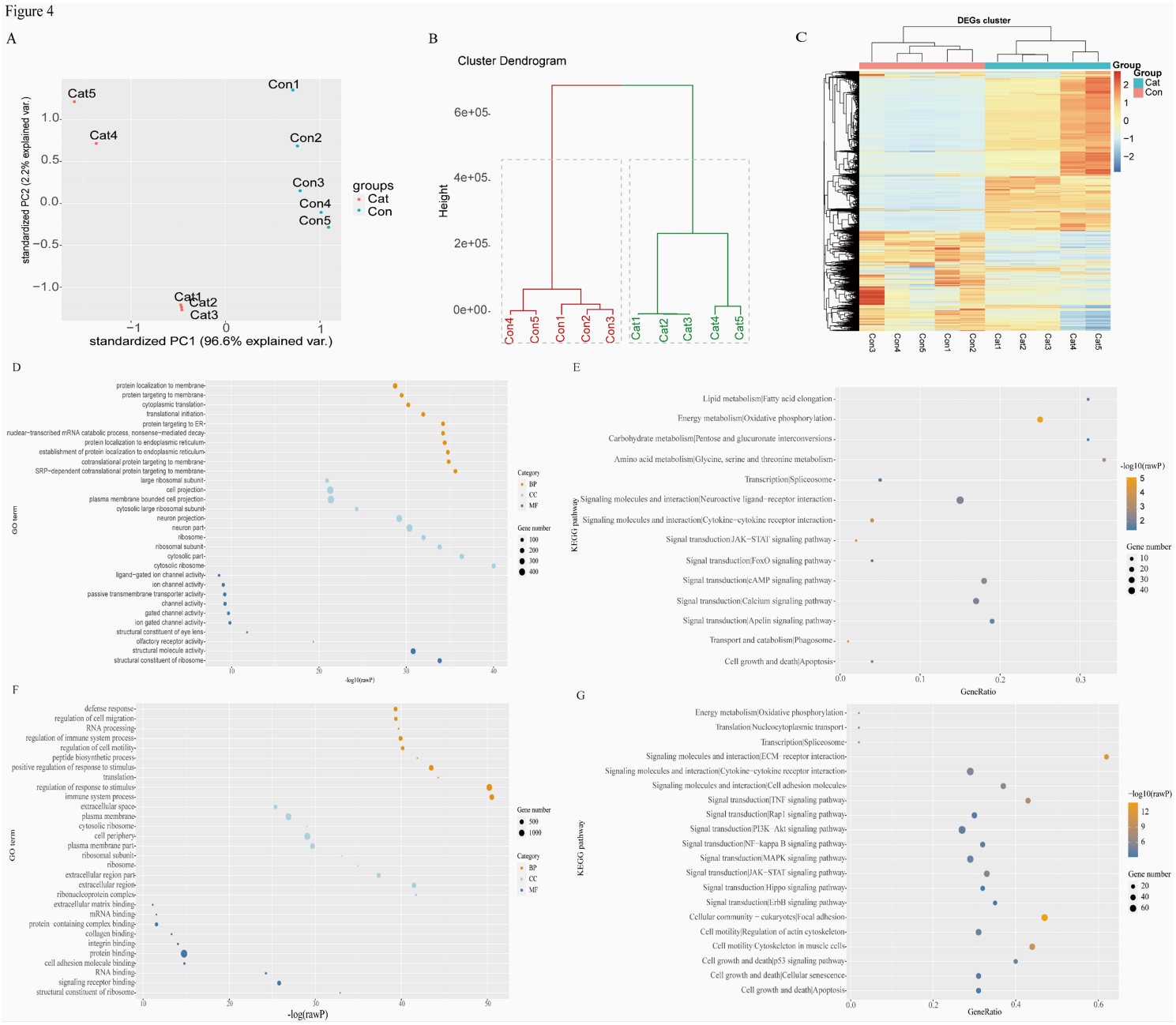


Figure 4

Transcriptomic analysis of lens from cataract and healthy *M. fortis*. (**A**) PCA analysis of all samples. (**B**) Cluster analysis of all samples. (**C**) Heatmap of DEGs in each group. The threshold for these data was $p < 0.05$ and | log2(fold-change) | > 1. (**D**) GO enrichment analysis of overlapping downregulated DEGs. GO analysis of predicted genes was performed according to cellular component (CC), biological process (BP) and molecular function (MF). (**E**) KEGG enrichment analysis of downregulated DEGs between cataract and healthy groups. (**F**) GO enrichment analysis of overlapping upregulated DEGs. (**G**) KEGG enrichment analysis of upregulated DEGs between cataract and healthy groups.

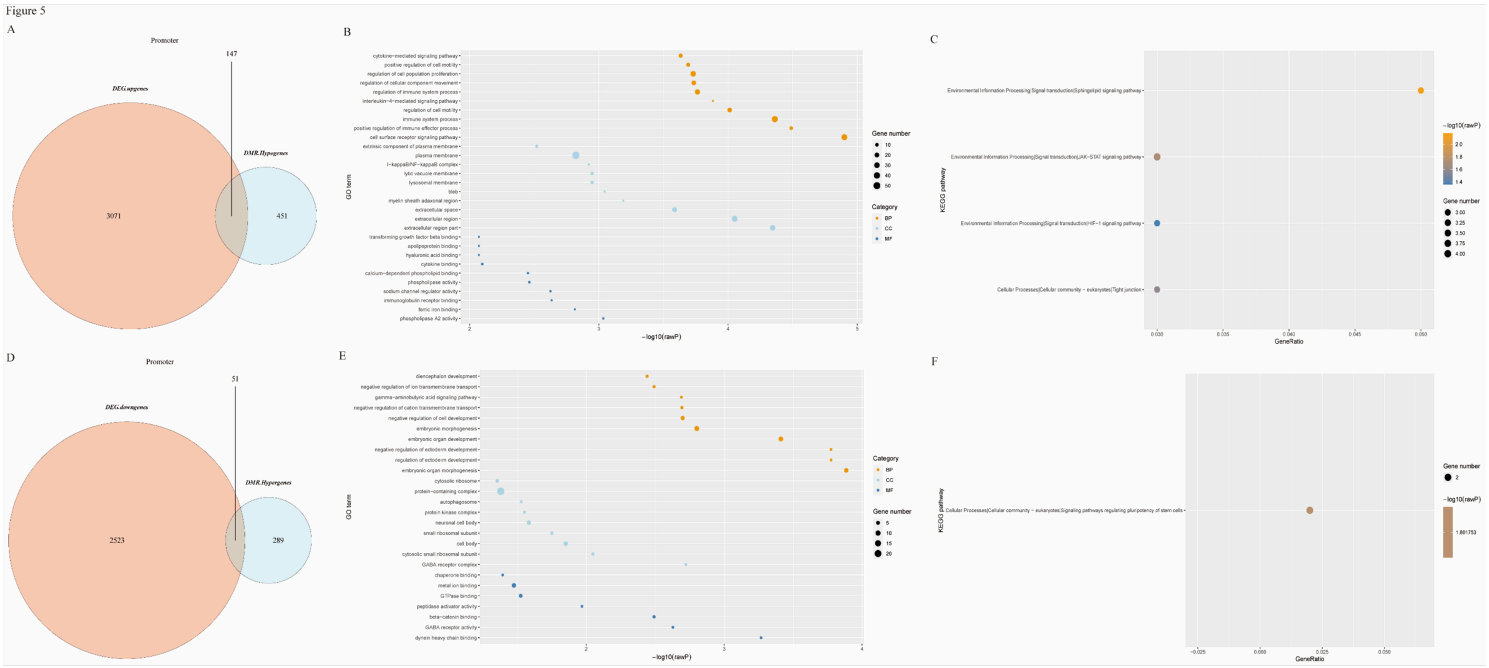


Figure 5

Integrative analysis of DMRs and genome-wide gene expression. (**A**) Venn diagram screening of upregulated DEGs with promoter hypomethylation. (**B** and **C**) GO and KEGG analysis of genes upregulated by promoter hypomethylation in cataract*M. fortis*. (**D**) Venn diagram screening of downregulated DEGs with promoter hypermethylation. (**E** and **F**) GO and KEGG analysis of genes downregulated by promoter hypermethylation in cataract group.

Figure 6

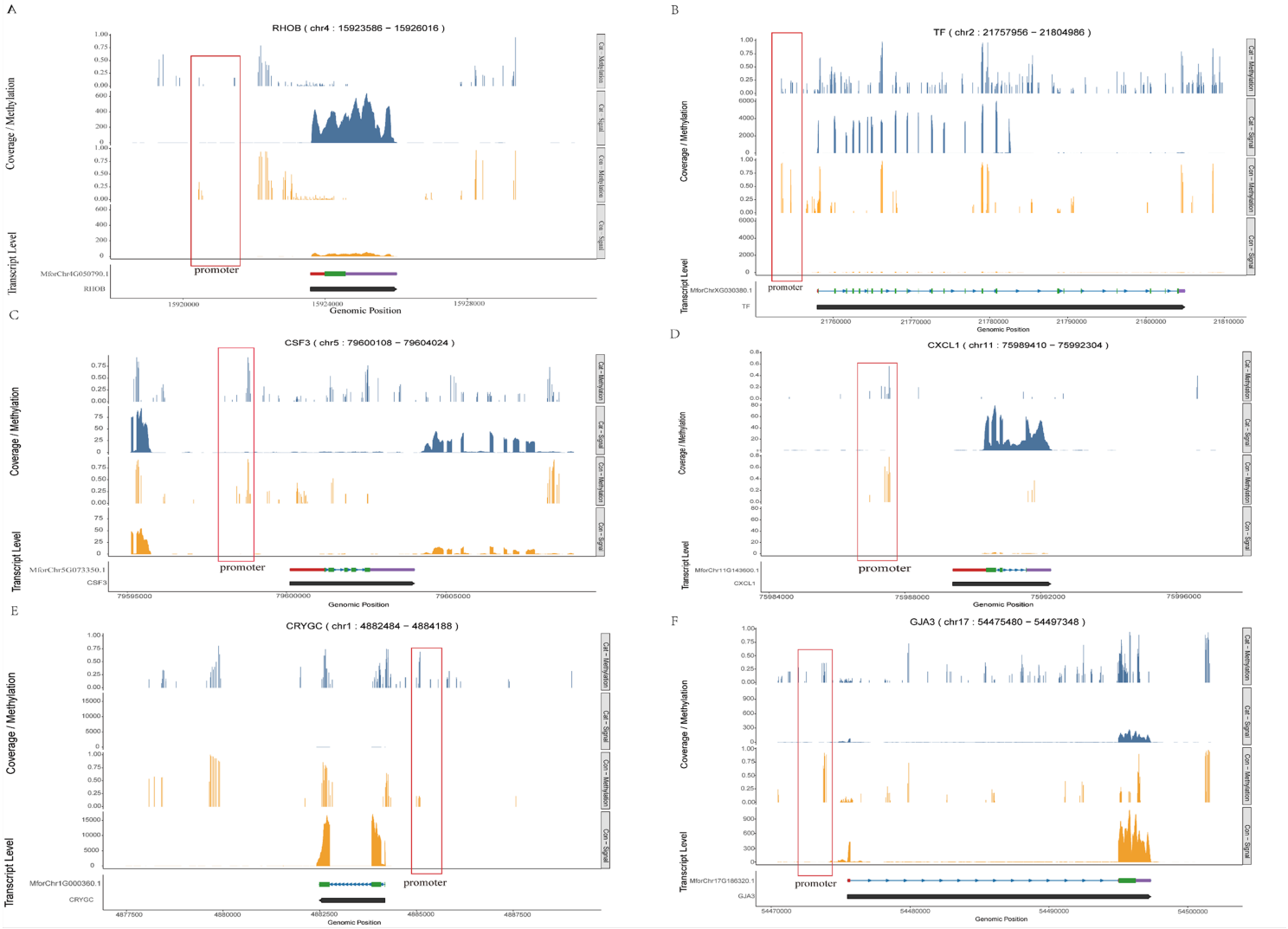


Figure 6

Integrative Genomics Viewer (IGV) was used to characterize epigenetic regulation of the identified genes. (**A-F**) The IGV results of *RHOB, TF, CSF3, CXCL1, CRYGC, GJA3* genes, respectively. The track labeled signal represents gene expression levels, while the methylation track displays methylation signals with values ranging from 0 to 1. The panel shows the transcript structure of the gene, red indicated the 5'UTR, green indicated the CDS, and purple indicated the 3'UTR.

Supplementary Files

This is a list of supplementary files associated with this preprint. Click to download.

- Table1.xlsx
- Table2.xlsx
- Table3.xlsx
- Table4.xlsx

- TableS1.xlsx